Creation of Cadmium Sulfide Nanostructures Using AFM Dip-Pen Nanolithography

Lei Ding,[†] Yan Li,*[,†] Haibin Chu,[†] Xuemei Li,[†] and Jie Liu*[,‡]

Key Laboratory for the Physics and Chemistry of Nanodevices, College of Chemistry and Molecular Engineering, Peking University, Beijing 100871, China, and Department of Chemistry, Duke University, Durham, North Carolina 27708, U.S.A.

Received: June 22, 2005; In Final Form: September 22, 2005

A dip-pen nanolithography (DPN) process capable of depositing nanoscaled structures of semiconducting CdS materials was developed by careful control of the reaction speed between the precursors. The new development expanded the scope of the powerful DPN process and provided more insight in the deposition mechanism. Features ranging from several hundreds of nanometers to sub-50 nanometers were generated and characterized. The effects of the surface property of the substrate, the relative humidity, the translating rate, and the temperature were systematically investigated. X-ray photoelectron spectroscopy (XPS) was used to verify the chemical composition of the patterns. In principle, this simple and convenient method should be applicable to deposit various metal sulfides on suitable substrates.

Introduction

The development of straightforward methods to create and organize sub-100 nm structures on surfaces is one of the greatest challenges facing researchers in the areas of nanoscience and nanotechnology.[1,2] It enables new possibilities in applications ranging from nano and molecular electronics, biomedicine, to catalysis.[1] Many lithography methods, such as electron-beam lithography,[3] photo lithography,[4] microcontact printing,[5] nanoimprint lithography,[6] scanning probe lithography (SPL),[7] and focused ion beam lithography (FIB),[8] were used to fabricate structures or patterns from micro- to nanoscale. Among these techniques, SPL is a unique approach to generate patterns on various substrates[7,9] using the tip of a scanning probe microscope (SPM) as the tool for structure creation. Among various SPL techniques, dip-pen nanolithography (DPN)[10,11] has attracted great attention as a direct-write method, in which an AFM tip is used to deliver materials directly to nanoscopic regions of a substrate. The AFM tip was first used for the patterning generation of octadecanethiols (ODT) on the mica surface in 1995.[7e] To date, DPN has been shown to be a powerful tool for the creation of microscale and nanoscale patterns of organic molecules,[9,12,13] polymers,[14,15] dendrimer,[16] biomolecules,[17−20] and inorganic molecules.[21−24]

Although the deposition mechanism and the role of the water meniscus formed spontaneously between the AFM tip and the substrate are still an issue of debate in the research field,[25] significant progress has been made in nanopatterning of biomolecules and organics by modulating interactions between molecules and the target surfaces.[11−14,17,18] However, successful examples of using DPN to fabricate nanopatterns of inorganic materials are relatively few, and it remains largely unexplored. Until now, pure metals[14,21−23,26,27] (Au, Pt, Pd, Ag, Cu, and maybe semimetals such as germanium) and metal oxides[24,28] are the only inorganic materials that have been successfully patterned by DPN. Therefore, it is important to explore new reactions of various inorganic materials for DPN deposition.

In this paper, we describe a well-controlled reaction for patterning cadmium sulfide (CdS) on mica and negatively charged silicon wafer. To the best of our knowledge, this is the first attempt for directly writing CdS nanopatterns using DPN. Cadmium sulfide is an important II−VI semiconductor with a band-gap of 2.42 eV at room temperature. It has potential applications in the fields of solar cells, light-emitting diodes, and sensors.[29] To deposit CdS using DPN, both Cd^{2+} and S^{2-} species are needed to be present between the AFM tip and the substrate. However, the reaction between Cd^{2+} and S^{2-} precursors is so fast that they are not suitable for the DPN process, which requires the precursor to be reactive during the entire period of the deposition process. In our approach, thioacetamide (CH_3CSNH_2, TAA) rather than the normally used Na_2S or $(NH_4)_2S$ is chosen as the sulfide source to react with Cd^{2+}. In the DPN process, TAA releases H_2S gradually when dissolved in the water meniscus formed between the AFM tip and the substrate through the following reaction:[30]

$$CH_3CSNH_2 + 2H_2O \rightarrow CH_3COONH_4 + H_2S$$

Then, H_2S reacts with Cd^{2+} ions to form CdS, and finally, the produced CdS deposits on the substrate to form nanopatterns along with the movement of the tip. Figure 1 illustrates the DPN process for the patterning of the CdS.

Experimental Section

1. Substrate Preparation. p-Type Si(111) wafers were cut into 0.5 cm × 0.5 cm pieces for the following treatment.

Preparation of OH-Terminated Silicon Wafer. After being ultrasonicated with isopropyl alcohol for 5 min and rinsed with Milli-Q water, the wafers were cleaned in 100 °C piranha solution (H_2SO_4/H_2O_2 = 7/3, v/v) for 30 min, rinsed with water, and blownn dry with high-purity nitrigon.

Preparation of H-Terminated Silicon Wafer. After being cleaned by piranha solution and rinsed with water, the wafer was dipped in the 5% aqueous HF solution to remove the silicon oxide layer, and rinsed with water. Normally, the wafer was used for lithography within several hours of oxide removal.

* E-mail: yanli@pku.edu.cn (Y.L.); jliu@chem.duke.edu (J.L.).
† Peking University.
‡ Duke University.

10.1021/jp053389r CCC: $30.25
Published on Web 10/26/2005

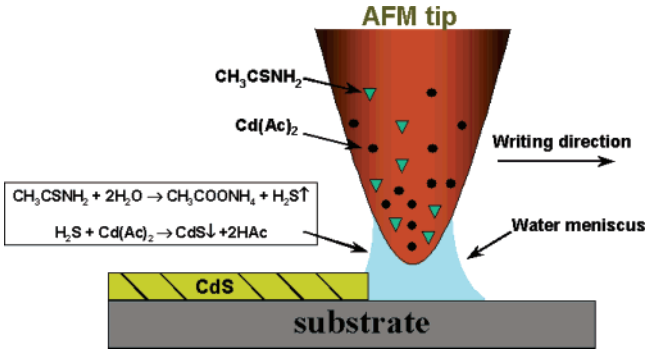

Figure 1. Schematic diagram of the experimental setup.

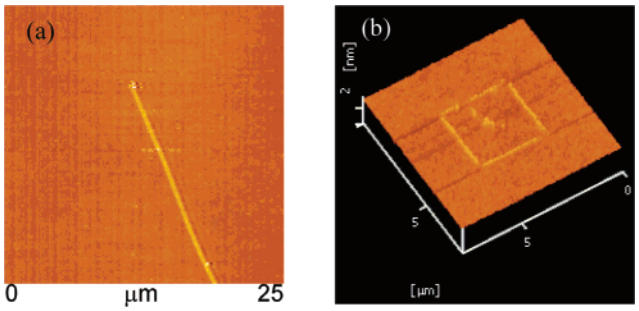

Figure 2. Two- and three-dimensional topographic AFM images of CdS nanopattern drawn on the mica surface (a) and piranha solution generated silicon surface (b). The CdS nanoline on the mica surface, with the height of about 2 nm and width of 300 nm, was drawn at a writing speed of 60 nm/s under the relative humidity of 48%. The pattern was imaged by contact-mode AFM with the scanning rate of 2.4 Hz and 256 lines per scan direction. The CdS nanopattern on the piranha solution generated silicon surface, with the height of about 0.7 nm and width of 105 nm, was drawn at a writing speed of 100 nm/s under the relative humidity of 40%. The patterns are imaged by a tapping-mode AFM with the scanning rate of 1 Hz and 256 lines per scan direction.

Preparation of APS Self-Assembly Monolayer (SAM). After being treated with piranha solution, the silicon wafers were soaked in 0.1% (w/w) aminopropyl trimethoxysilane (APS, 97%, Aldrich) alcohol solution for 1 h to form SAM on the surface of silicon wafer. Then, the sample with APS SAM was heated at 120 °C for 30 min to improve the stability of the SAM. At last, the wafers were sonicated in Milli-Q water for 1−2 min to clean the surface.

2. Coating AFM Tip. The "ink" used in our experiments is freshly mixed ethanol solution of $Cd(Ac)_2$ (1 mM) and TAA (1 mM). Standard Si cantilever was immersed in the as-prepared "ink" for 2−20 s and dried in air.

3. DPN Procedure and AFM Imaging. A SPA3800 SPM (Seiko Instrument Inc.) equipped with a 100 μm scanner was used for DPN and AFM imaging. In contact mode, cantilever A of NSC11 AFM tip (MikroMasch) was used (force constant $k = 3.0$ N m^{-1}). In noncontact mode, cantilever B was used (force constant $k = 48$ N m^{-1}). The relative humidity, measured with a digital hygrometer, could be well-controlled and maintained between 25% and 65% by a humidifier and a dehumidifier. After deposition, AFM images were taken using normally the same cantilever in contact-mode AFM at a relatively high scanning rate of 2.4 Hz. However, for the very tiny nanofeatures, tapping-mode AFM was used to image (Figure 2b). All images were recorded in height mode.

4. X-ray Photoelectron Spectroscopy (XPS) Characterization. The "ink"-coated tip was brought into contact with the substrate for 15 s to deposit a large amount of spots on the mica surface. Each tip was used to generate no more than three spots and subsequently cleaned for another ink-coating procedure. An area of about 300 μm × 300 μm on the mica surface has been modified with the CdS spots for XPS characterization. The XPS data were collected in an AXIS-Ultra instrument from Kratos Analytical using monochromatic Al Kα radiation (225 W, 15 mA, 15 kV) and low-energy electron flooding for charge compensation. To compensate for surface charge effects, binding energies were calibrated using C1s hydrocarbon peak at 284.8 eV.

Results and Discussion

Several factors have been found to be crucial for the fabrication of CdS nanopatterns on the substrates, which will be explained in the following section.

Effect of Surface Charge. It is widely accepted that surface affinity of the target materials is essential in DPN.[11,15,16] Thus, the property of the substrate surface is an important factor for DPN processing. In our experiment, it was observed that freshly cleaved mica or silicon surface newly treated with piranha solution are much more suitable for the deposition of CdS nanopatterns. Figure 2 shows the CdS nanopatterns drawn on the surfaces of mica and silicon wafer. We attribute the phenomena to the affinity between nanosized CdS and the surfaces. We proposed the following mechanism for the deposition: When the precursors are dissolved in the water meniscus, $Cd(Ac)_2$ ionizes immediately, but TAA decomposes very slowly. Hence, the formation of CdS is carried out under the condition of excessive Cd^{2+}. Because of the existence of dangling bonds at the surface of the CdS nanospecies, extra Cd^{2+} ions tend to absorb on them and make them positively charged. On the other hand, freshly cleaved mica contains surface anions in air and in water,[31] and piranha solution generates negatively charged silicon surface.[32] Therefore, the static interaction between the negatively charged substrate surface and the positively charged CdS nanospecies leads to the deposition of CdS onto the substrate surface. We also tried to draw CdS on the H-terminated silicon surface and positively charged silicon surface modified by APS SAMs under similar conditions, but no CdS nanopattern could be obtained. Furthermore, negatively charged silicon surface generated by another method has successfully been used as the substrate for CdS pattern generation (see Supporting Information).

Effect of Sulfide Source. The use of TAA as sulfide source is another important factor for the process. If Na_2S or $(NH_4)_2S$ were used as sulfide sources in experiment, the speeds of CdS formation are found to be too fast even for the "inking" of the AFM tip. Even at the concentration of 1×10^{-4} M, the solutions become turbid in less than 1 s because of the formation of CdS. The rapid formation of CdS makes it difficult to "ink" the tip. The formation of CdS also makes the "sharp" tip lose its functionalities as a probe for scanning or DPN. Yet, when the concentration of the mixed ethanol solution of $Cd(Ac)_2$ and TAA is increased to 1×10^{-3} M for each precursor, the solution is transparent over 1 min. One minute is enough to "ink" the tip with $Cd(Ac)_2$ and TAA. The fast evaporating rate of ethanol solution will make the tip dry quickly, which baffled the reaction between the $Cd(Ac)_2$ and TAA. As a result, the tip can be coated uniformly without the formation CdS particles on the tip. Consequently, the use of TAA as sulfide source makes the reaction speed controlled to a proper speed, and the formation of CdS is confined within the water meniscus and/or on the substrate surface.

Temperature Dependence. Temperature is known to be an important factor in the DPN process. For the DPN of "soft"

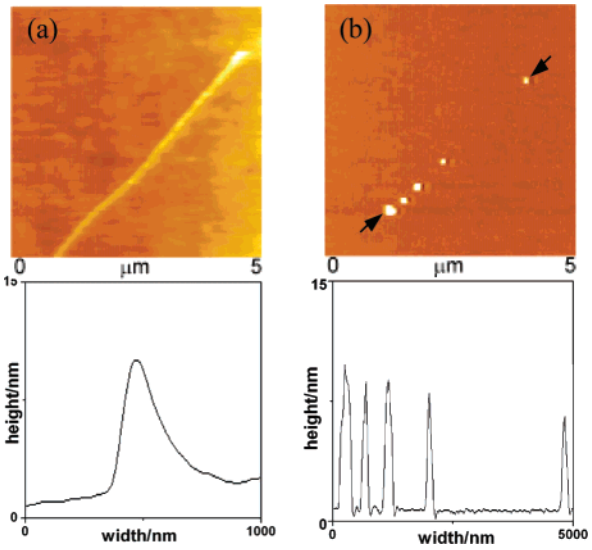

Figure 3. AFM images illustrating the temperature dependence of the formation of CdS patterns by DPN. Parts a and b separately show the patterns we drew in succession at 20 and 5 °C. The upper are the topographic images; the lower are the cross-section profiles. (In part b, the cross-section is between the arrows in the AFM image.) The translation speed was 15 nm/s, and the relative humidity was 40%. The same tip has been used for patterns (a) and (b) generation. The patterns are imaged by contact-mode AFM with the scanning rate of 2.4 Hz and 256 lines per scan direction.

materials such as organic or biomolecules, temperature mainly affects the solubility and diffusion rate of the molecules and consequently influences the size of the resultant nanopatterns.[25a,d,e] However, the reaction rate of TAA with water to release H_2S is highly dependent on temperature.[33] So, temperature is a much more crucial factor in our process to deposit CdS. In our experiments, the temperature not only affects the solubility and diffusion of the precursors, it may also affect the DPN process by changing the formation speed of CdS. We have performed the DPN process at various temperatures on mica surfaces. The results are shown in Figure 3. At 5 °C, no desired nanopatterns could be obtained, no matter at what humidity the DPN process was performed. When the temperature was between 20 and 25 °C, we were able to get CdS nanopatterns at a wide range of humidity conditions. However, it became difficult again at temperatures higher than 30 °C to obtain well-controlled nanopatterns. Such strong temperature dependence cannot be easily explained by the diffusion of the materials alone; the effect on the reaction rate between the precursor and water need to be taken into account. In all of the following experiments, the temperature range is controlled between 20 and 25 °C.

Translating Rate Dependence. Figure 4 shows CdS patterns drawn at rates of 120 nm/s (position A), 60 nm/s (position B), and 30 nm/s (position C) on the mica surface with the relative humidity of 40% and the temperature of 25 °C. As shown in the figure, the increase of the translating rates decreases the sizes of the created patterns. Line C drawn at 30 nm/s is with the height of about 55 nm and width of 280 nm, and line B drawn at 60 nm/s is with the height of about 40 nm and width of 250 nm. When the rate was 120 nm/s, we could not create CdS nanopatterns with continuous morphology. Only at the beginning of writing on position A were some CdS nanoparticles obtained because of the relatively longer contact time with the mica. We believe that a high translation rate will inhibit the formation of a stable water meniscus and thus inhibit the deposition process. More effect of the stability of the water meniscus is discussed in the following section.

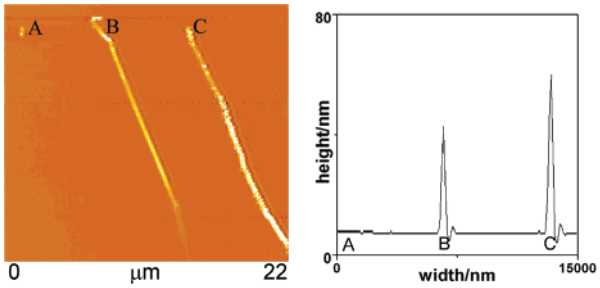

Figure 4. The cross-section topographic AFM image and the height profile of CdS nanopattern drawn sequentially on mica surface at the different translating rates. To eliminate the effect of the amounts of reactants on the moving tip, the patterns were generated from the highest rate of 120 nm/s (spot A) to the lower rate of 60 nm/s (spot B) and 30 nm/s (spot C). The line C is with the height of about 60 nm and width of 280 nm, and the line B is with the height of about 40 nm and width of 250 nm. As the translating rates increase, the sizes of the patterns decrease. When the rate was up to 120 nm/s, we could not obtain CdS nanopatterns with continuous morphology. The relative humidity was 40%, and the temperature was 25 °C. The patterns are imaged by a contact-mode AFM with the scanning rate of 2.4 Hz and 256 lines per scan direction.

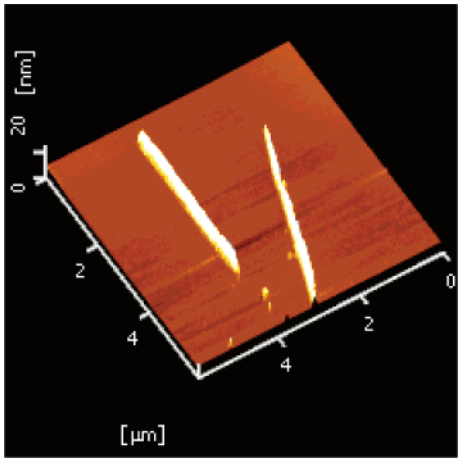

Figure 5. The three-dimensional topographic AFM image showing the CdS pattern generated at the relative humidity of 55% and the translation speed of 120 nm/s. The temperature was 25 °C. The pattern is imaged by contact-mode AFM with the scanning rate of 2.4 Hz and 256 lines per scan direction.

Humidity Effect. Former research shows that different molecules exhibit different dependence on relative humidity in DPN.[11,25a,c,d,f] We found that relative humidity acts as a key factor in our deposition process. In Figure 5, we have demonstrated that, as the translation rate increased to 120 nm/s, there was no CdS line formed on the mica at the humidity of 40%. Yet, the situation was different when the humidity was increased to 55%. Figure 5 shows the CdS lines we drew under the humidity of 55% with the translation rate of 120 nm/s. The same tip has been used for the pattern generation in both Figures 4 and 5. However, when the humidity is too high (>65%), it is difficult to get any desired CdS nanolines on mica. Figure 6 illustrates the line generated under the humidity of 65% at the translation rate of 120 nm/s. We found that, along with the direction of the tip movement (parallel with the direction of the arrow), the width of the pattern is becoming larger even when we used a relatively high translation speed (120 nm/s). Yet, the longest writing time is achieved at the humidity of 40% and is about 15 min without any change of the tip. We also found that, if the humidity was below 30%, no nanopatterns of CdS could be created on the surface of mica. These results shown that a proper humidity level was crucial to DPN of CdS.

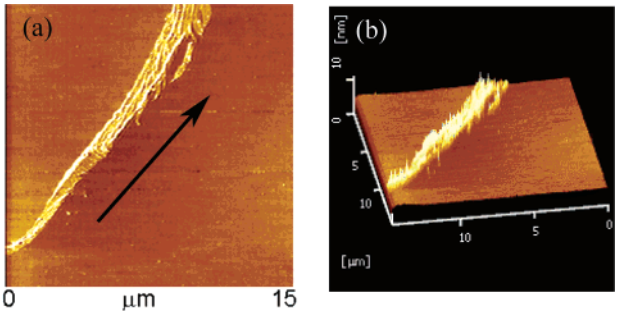

Figure 6. The two- (a) and three- (b) dimensional topographic images of the pattern generated under the relative humidity of 65%. The tip moved along the direction of the arrow shown in the image (a). The precoated contact-mode AFM tip translated across the mica surface at a rate of 120 nm/sm and the temperature was 25 °C. The patterns are imaged by contact-mode AFM with the scanning rate of 2.4 Hz and 256 lines per scan direction.

Finally, we used XPS to verify that the nanofeatures deposited on the mica surface in the DPN process were composed of CdS (see Supporting Information).

Conclusion

CdS nanopatterns have been fabricated directly on mica and negatively charged silicon surfaces with the DPN technique based on a reaction between thioacetamide and cadmium acetate. The morphology of these CdS nanopatterns is affected by the surface property of the substrate, the humidity, the translating rate, and the temperature. The use of thioacetamide as the precursor of H_2S plays the critical role in this process. It makes the originally violent reaction controllable and compatible with the DPN process. The experiments demonstrated a general idea of fabricating nanopatterns of metal sulfide and other inorganic materials by DPN. By carefully designing the reactions, DPN can be a powerful technique for on-site, one-step nanofabrication. Various kinds of nanopatterns based on different materials can be fabricated by DPN.

Acknowledgment. The authors would like to thank Prof. Nianzu Wu and Mr. Jinglin Xie for helpful discussion on the XPS results. This research was supported by NSFC, MOE, MOST, and NCNST of China.

Supporting Information Available: Supporting materials about the images of CdS nanofeatures being patterned on different surfaces. This material is available free of charge via the Internet at http://pubs.acs.org.

References and Notes

(1) Duan, X.; Huang, Y.; Cui, Y.; Liber, C. M. Nanowire nanoelectrics assembled from the bottom-up. In *Molecular Nanoelectronics*; Reed, M. A., Lee, T., Eds.; American Scientific Publishers: Stevenson Ranch, CA, 2003; pp 199−227.

(2) Drexler, K. E. *Engines of creation. The coming era of nanotechnology*; Anchor Books Doubleday: New York, 1986

(3) Wallraff, G. M.; Hinsberg, W. D. *Chem. Rev.* **1999**, *99*, 1801.

(4) Nicolau, D. V.; Tauguchi, T.; Taniguchi, H.; Yoshikawa, S. *Langmuir* **1998**, *14*, 1927

(5) (a) Xia, Y.; Whitesides, G. M. *Angew. Chem., Int. Ed. Engl*. **1998**, *37*, 550. (b) Xia, Y.; Rogers, J. A.; Paul, K. E.; Whitesides, G. M. *Chem. Rev.* **1999**, *99*, 1823.

(6) Chou, S. Y. *MRS Bull.* **2001**, *26*, 512.

(7) (a) Liu, G. Y.; Xu, S.; Qian, Y. *Acc. Chem. Res.* **2000**, *33*, 457. (b) Kramer, S.; Fuierer, R. R.; Gorman, C. B. *Chem. Rev*. **2003**, *103*, 4367. (c) Nyffenegger, R. M.; Penner, R. M. *Chem. Rev.* **1997**, *97*, 1195. (d) Quate, C. F. *Surf. Sci*. **1997**, *386*, 259. (e) Jaschke, M.; Butt, H.-J. *Langmuir* **1995**, *11*, 1061

(8) Bergman, A. A.; Buijs, J.; Herbig, J.; Mathes, D. T.; Demarest, J. J.; Wilson, C. D.; Reimann, C. T.; Baragiola, R. A.; Hull, R.; Oscarsson, S. O. *Langmuir* **1998**, *14*, 6785.

(9) (a) Eigler, D. M.; Schweizer, E. K. *Nature (London)* **1990**, *344*, 524−526. (b) Crommie, M. F.; Lutz, C. P.; Eigler, D. M. *Science* **1993**, *262*, 218−220. (c) Mo, Y. W. *Science* **1993**, *261*, 886−888. (d) Falvo, M. R.; Taylor, R. M., II; Helser, A.; Chi, V.; Brooks, F. P., Jr.; Washburn, S.; Superfine, R. *Nature (London)* **1999**, *397*, 236−238.

(10) Hong, S. H.; Zhu, J.; Mirkin, C. A. *Science* **1999**, *286*, 523−525.

(11) (a) Piner, R. D.; Zhu, J.; Xu, F.; Hong, S. H.; Mirkin, C. A. *Science* **1999**, *283*, 661−663. (b) Ginger, D. S.; Zhang, H.; Mirkin, C. A. *Angew. Chem., Int. Ed.* **2004**, *43*, 30

(12) Hong, S. H.; Zhu, J.; Mirkin, C. A. *Science* **1999**, *286*, 523−525.

(13) (a) Hang, S. H.; Mirkin, C. A. *Science* **2000**, *288*, 1808−1811. (b) Bullen, D.; Chung, S. W.; Wang, X. F.; Zou, J.; Mirkin, C. A.; Liu, C. *Appl. Phys. Lett.* **2004**, *84*, 789. (c) Ivanisevic, A.; Mirkin, C. A. *J. Am. Chem. Soc.* **2001**, *123*, 7887−7889.

(14) Maynor, B. W.; Filocamo, S. F.; Grinstaff, M. W.; Liu, J. *J. Am. Chem. Soc*. **2002**, *124*, 522−523.

(15) Lim, J. H.; Mirkin, C. A. *Adv. Mater*. **2002**, *14*, 1474.

(16) McKendry, R.; Huck, W. T. S.; Weeks, B.; Florini, M.; Abell, C.; Rayment, T. *Nano Lett*. **2002**, *2*, 713.

(17) Wilson, D. L.; Martin, R.; Hong, S.; Cronin-Golomb, M.; Mirkin, C.; Kaplan, D. *Proc. Natl. Acad. Sci. U.S.A.* **2001**, *98*, 13660−13664.

(18) Lee, K.; Park, S.; Mirkin, C. A.; Smith, J. C.; Mrksich, M. *Science* **2002**, *295*, 1702−1705.

(19) Demers, L. M.; Ginger, D. S.; Park, S. J.; Li, Z.; Chung, S. W.; Mirkin, C. A. *Science* **2002**, *296*, 1836.

(20) Lu, J.-h.; Li, H.-k.; An, H.-j.; Wang, G.-h.; Wang, Y.; Li, M.-q.; Zhang, Y.; Hu, J. *J. Am. Chem. Soc.* **2004**, *126*, 11136.

(21) Li, Y.; Maynor, B. W.; Liu, J. *J. Am. Chem. Soc*. **2001**, *123*, 2105−2106.

(22) Maynor, B. W.; Li, Y.; Liu, J. *Langmuir* **2001**, *17*, 2575−2578.

(23) Porter, L. A.; Choi, H. C.; Schmeltzer, J. M.; Ribbe, A. E.; Elliott, L. C. C.; Buriak, J. M. *Nano Lett*. **2002**, *2*, 1369.

(24) Gundiah, G.; John, N. S.; Thomas, P. J.; Kulkarni, G. U.; Rao, C. N. R. *Appl. Phys. Lett*. **2004**, *84*, 5341.

(25) (a) Schwartz, P. V. *Langmuir* **2002**, *18*, 4041. (b) Sheehan, P. E.; Whitman, L. J. *Phys. Rev. Lett.* **2002**, *88*, 156104. (c) Weeks, B. L.; Noy, A.; Miller, A. E.; De Yoreo, J. J. *Phys. Rev. Lett.* **2002**, *88*, 255505. (d) Rozhok, S.; Piner, R.; Mirkin, C. A. *J. Phys. Chem. B* **2003**, *107*, 751. (e) Sheehan, P. E.; Whitman, L. J.; King, E. P.; Nelson, B. A. *Appl. Phys. Lett*. **2004**, *85*, 1589. (f) Peterson, E.; Weeks, B. L.; De Yoreo, J. J.; Schwartz, P. V. *J. Phys. Chem. B* **2004**, *108*, 15206.

(26) Thomas, P. J.; Kulkarni, G. U.; Rao, C. N. R. *J. Mater. Chem.* **2004**, *14*, 625.

(27) Zhang, H.; Lee, K. B.; Li, Z.; Mirkin, C. A. *Nanotechnology* **2003**, *14*, 1113.

(28) Su, M.; Liu, X. G.; Li, S. Y.; Dravid, V. P.; Mirkin, C. A. *J. Am. Chem. Soc*. **2002**, *124*, 1560

(29) Maoz, R.; Frydman, E.; Cohen, S. R.; Sagiv, J. *Adv. Mater*. **2000**, *12*, 424.

(30) Li, Y.; Xu, D. S.; Zhang, Q.; Chen, D. P.; Huang, F. Z.; Xu, Y. J.; Guo, G. L.; Gu, Z. N. *Chem.* Mater. **1999**, *11*, 3433−3435.

(31) Ducker, W. A.; Wanless, E. J. *Langmuir* **1999**, *15*, 160−168.

(32) (a) Chrisey, L. A.; G Lee, G. U.; O'Ferrall, C. E. *Nucleic Acids Res*. **1996**, *24*, 3031. (b) Moriguchi, I.; Teraoka, Y.; Kagawa, S.; Fendler. *Chem. Mater*. **1999**, *11*, 1603. (c) Im, H. J.; Kwon, P. O.; Kim, H. J.; Lee, S. H. *Macromolecules* **2000**, *33*, 9606.

(33) (a) Butler, E. A.; Peters, D. G.; Swift, E. H. *Anal. Chem.* **1958**, *30*, 1379. (b) Yamaguchi, K.; Yoshida, T.; Sugiura, T.; Minoura, H. J. *Phys. Chem. B* **1998**, *102*, 9677.